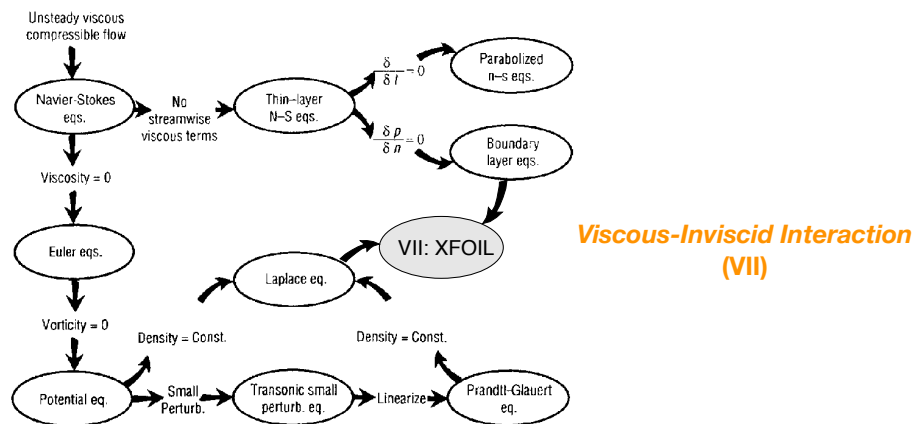
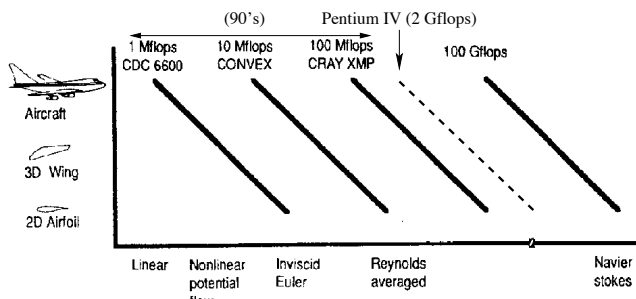


# Airfoil analysis and design

## Hierarchy of flow models with simplifying assumptions



## Flow model complexity versus cost of analysis



# Airfoil analysis versus design

The aerospace engineer could face an aerodynamical problem in two forms:

### 1. Analysis: the Direct Problem

*What are the aerodynamic characteristics of a given airfoil shape?*

### 2. Design: the Inverse Problem

*What is the airfoil shape that leads to given aerodynamic characteristics?*

We will look at the tools for both tasks.

The basic presumption of most wing analysis and design is that the flow local to each section of the wing is approximately 2D. This enables us to focus on 2D profile design more-or-less independently of finite-wing effects.

Drela (1990):

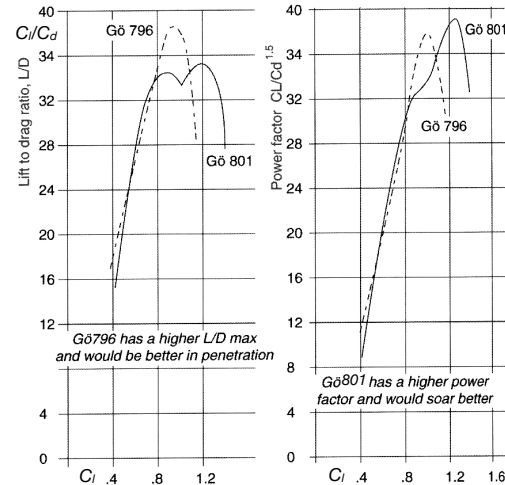
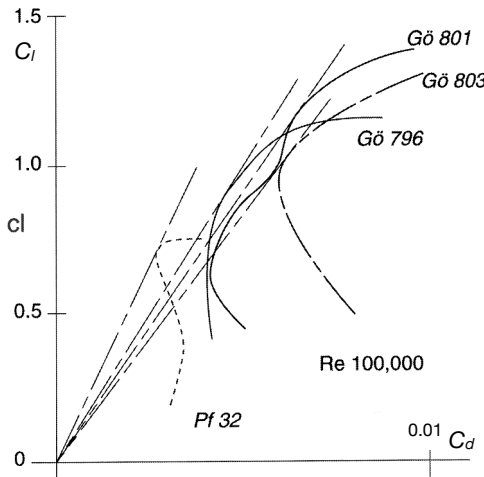
*... resolving wing profile design conflicts is far more effective when done at the 2D level.*

Liebeck (1990):

*Stated in simple form, the minimum requirements for an airfoil are that it is non-re-entrant, has a rounded leading edge, and has a pointed trailing edge.*

## How do we assess airfoil performance?

A broad-brush approach looks at the airfoil performance as a whole, based on the drag polar and measures derived from this — e.g.  $(C_l/C_d)_{\max}$ ,  $(C_l^{1/2}/C_d)_{\max}$ ,  $(C_l^{3/2}/C_d)_{\max}$ . [Used to compare/select airfoils.](#)



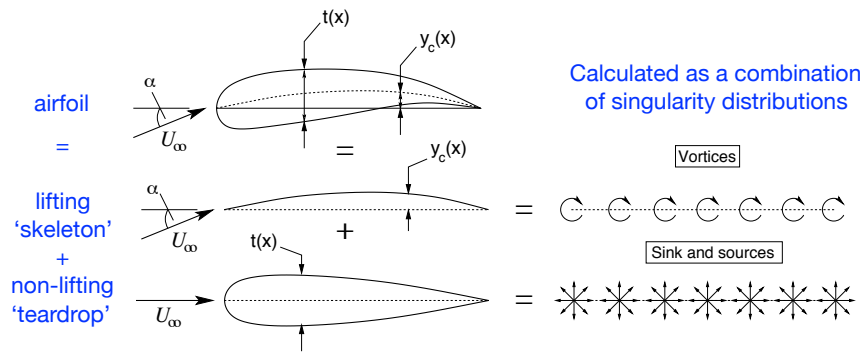
Finer-scale measures look more carefully to the underlying causes of specific performance aspects, e.g.:

1. Low drag ( $C_d$ ) over design lift coefficient range ( $C_l$ );
2. Turbulent transition and drag (for laminar flow airfoils);
3. Mach number sensitivity (transonic drag rise);
4. Reynolds number sensitivity;
5. Simple flap/aileron effects;
6. Surface waviness tolerance (to transition).

[Used in airfoil design.](#)

## Inviscid methods for airfoil analysis and design

# Thin airfoil theory



Calculated as a combination of singularity distributions

For simplicity it is here assumed that the vorticity  $\gamma$  lies along the chord line **but** it has the correct strength to match the flow to the mean camber line.

## Vortex-sheet analysis for lifting skeleton

Linearize,  $\alpha$  small

$$u = U_\infty + u'$$

$$v = U_\infty \alpha + v'$$

No flow normal to mean camber line:

$$U_\infty \left( \alpha - \frac{dy_c}{dx} \right) + v' = 0$$

Assume potential flow

$$u' = \frac{\partial \phi}{\partial x}$$

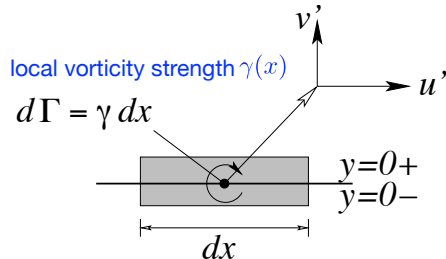
$$\nabla^2 \phi = 0$$

$$v' = \frac{\partial \phi}{\partial y}$$

— superposition is valid

## Lifting solution — direct method — 1

Calculate  $C_p(x)$  for a cambered airfoil skeleton with zero thickness,  $y=y_c(x)$ . (Say chord  $c=1$ .)



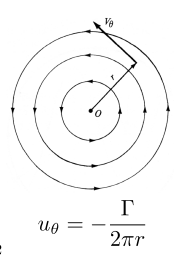
The aerodynamic characteristics are

$$\left. \begin{aligned} u'(x, 0\pm) &= \pm \frac{\gamma}{2} \\ v'(x, 0) &= -\frac{1}{2\pi} \int_0^c \gamma(\xi) \frac{d\xi}{x-\xi} \end{aligned} \right\} \text{via Biot-Savart}$$

$$C_p = \mp \frac{\gamma}{U_\infty} \quad \text{recall} \quad C_p = 1 - \left( \frac{U}{U_\infty} \right)^2$$

$$C_l = \frac{2}{U_\infty c} \int_0^c \gamma(\xi) d\xi \quad = 1 - \left( \frac{U_\infty + u'}{U_\infty} \right)^2$$

recall for a discrete vortex



The strength per unit length  $\gamma(x)$  of the distribution of vorticity along the chord line is now obtained by solving the flow tangency condition

$$U_\infty \left( \alpha - \frac{dy_c}{dx} \right) + v'(x) = 0; \quad \text{with} \quad \gamma(1) = 0$$

Kutta condition, i.e.  $u'=0$  at TE

The final equation is

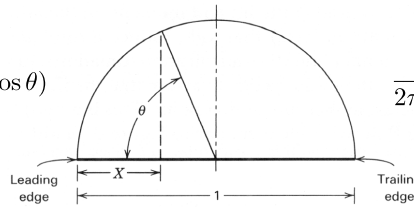
$$U_\infty \left( \alpha - \frac{dy_c}{dx} \right) - \frac{1}{2\pi} \int_0^1 \gamma(\xi) \frac{d\xi}{x-\xi} = 0; \quad \text{with} \quad \gamma(1) = 0$$

this has to be solved for  $\gamma(x)$  given the shape  $y_c$ .

## Lifting solution – direct method – 2

**Solution:** (by Betz)

Apply the mapping  $x = \frac{1}{2}(1 - \cos \theta)$



$$\frac{1}{2\pi U_\infty} \int_0^\pi \frac{\gamma(\theta) \sin \theta d\theta}{\cos \theta - \cos \theta(x)} = \alpha - \frac{dy_c(x)}{dx}$$

The vorticity distribution at  $\alpha \neq 0$  is singular like  $1/x$ , and is assumed to have a Fourier-type expansion

$$\gamma(x) = 2U_\infty \left( A_0 \frac{1 + \cos \theta}{\sin \theta} + \sum_{n=1}^{\infty} A_n \sin n\theta \right)$$

Use the relationships

$$\frac{1}{2} [\cos(n-1)\theta - \cos(n+1)\theta] = \sin n\theta \sin \theta \quad \text{and} \quad \int_0^\pi \frac{\cos n\theta d\theta}{\cos \theta - \cos \theta(x)} = \pi \frac{\sin n\theta(x)}{\sin \theta(x)}$$

to obtain

$$A_0 - \sum_{n=1}^{\infty} A_n \cos n\theta = \alpha - \frac{dy_c(x)}{dx}$$

Multiply both sides by  $\cos n\theta$ , integrate from 0 to  $\pi$ , obtain  $A_n$  as

$$A_0 = \alpha - \frac{1}{\pi} \int_0^\pi \frac{dy_c(\theta)}{dx} d\theta \quad A_n = \frac{2}{\pi} \int_0^\pi \frac{dy_c(\theta)}{dx} \cos n\theta d\theta$$

So for any camber line we can obtain the full set of coefficients.

## Lifting solution – direct method – 3

Using the Kutta-Joukowski relationship  $L = \rho U_\infty \Gamma$

$$L = \int_0^1 \rho U_\infty \gamma(x) dx \quad \text{and} \quad M_{LE} = \int_0^1 \rho U_\infty \gamma(x) x dx$$

**Lift**

$$C_l = 2\pi A_0 + \pi A_1 \quad \text{and} \quad \boxed{\frac{\partial C_l}{\partial \alpha} = 2\pi}$$

**Moment**

$$C_{m_{LE}} = -\frac{\pi}{2} \left( A_0 + A_1 - \frac{A_2}{2} \right)$$

now using statics (and  $\alpha$  small,  $C_d=0$ ) we had  $C_{m_x} = C_{m_a} - C_l \left( \frac{x}{c} - \frac{a}{c} \right)$  so

$$C_{m_{c/4}} = \frac{\pi}{4} (A_2 - A_1) \quad (\text{independent of } \alpha).$$

(Zero for a symmetrical section. i.e.  $A_1=A_2$ .)

These are two fundamental results of thin-airfoil theory.

## Lifting solution – inverse method

Calculate the camber line  $y=y_c(x)$  that produces a given pressure distribution  $C_p(x)$ .

From

$$v'(x, 0) = -\frac{1}{2\pi} \int_0^c \gamma(\xi) \frac{d\xi}{x - \xi}$$

$$C_p = \mp \frac{\gamma}{U_\infty}$$

we have

$$v'(x) = -\frac{1}{2\pi} \int_0^c U_\infty C_p(\xi) \frac{d\xi}{x - \xi}$$

and the shape of the camber line is obtained by integration of the flow tangency equation

$$U_\infty \left( \alpha - \frac{dy_c}{dx} \right) + v'(x) = 0$$

as

$$y_c(x) = \alpha x + \int_0^x \frac{v'(\xi)}{U_\infty} d\xi$$

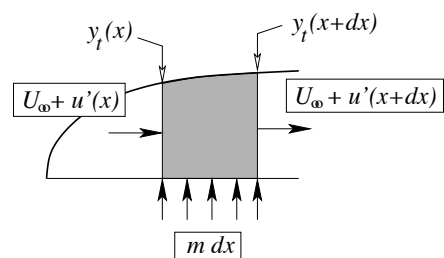
## Non-lifting solution – direct method

Calculate  $C_p(x)$  for a thin symmetric airfoil with a thickness distribution  $y=\pm y_t(x)/2$ .

(i) Airfoil surface is a streamline – by definition no flow crosses a streamline.

(ii) Flow internal to the streamline is created by source-sink distribution, local strength  $m$ .

$$\text{Conservation of mass: } m = 2U_\infty \frac{dy_t}{dx}$$



The aerodynamic characteristics are:

$$u'(x, 0) = \frac{U_\infty}{\pi} \int_0^c m(\xi) \frac{d\xi}{x - \xi}$$

$$v'(x, 0\pm) = \pm \frac{m}{2}$$

$$C_p = -\frac{2u'}{U_\infty}$$

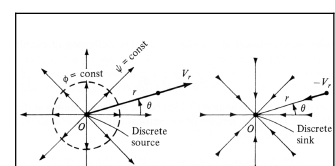
For instance, for an elliptic airfoil:

$$y_t = \pm t \sqrt{x - (c - x)}$$

$$\frac{dy_t}{dx} = \pm \frac{t}{2} \frac{c - 2x}{\sqrt{x(c - x)}}$$

$$C_p = -2t$$

Recall for a discrete source or sink:



$$u_r = \pm \frac{\Lambda}{2\pi r}$$

## Non-lifting solution — inverse method

Calculate thickness distribution  $y_t(x)$  that gives  $C_p(x)$ .

$$\text{Recall: } C_p = -\frac{2u'}{U_\infty}$$

This amounts to solving the equation:

$$C_p(x) = -\frac{2}{\pi} \int_0^c \frac{dy_t(\xi)}{dx} \frac{d\xi}{x-\xi}$$

$$u'(x, 0) = \frac{U_\infty}{\pi} \int_0^c \frac{dy_t(\xi)}{dx} \frac{d\xi}{x-\xi}$$

which can be done using Fourier series expansions for both  $y_t$  and  $C_p$  or, using a result by Betz, by direct integration of

$$\frac{dy_t}{dx} = \frac{1}{2\pi} \int_0^c C_p(x) \sqrt{\frac{\xi(c-\xi)}{x(c-x)}} \frac{d\xi}{x-\xi}$$

### Riegels' correction

The velocity distribution given by the theory,

$$\frac{u}{U_\infty} = 1 + \frac{1}{\pi} \int_0^c \frac{dy_t(\xi)}{dx} \frac{d\xi}{x-\xi}$$

is very inaccurate near rounded LEs, where  $dy_t/dx \rightarrow \infty$ , as then does  $u$ .

Riegels proposed a correction for the velocity which works for thicker airfoils

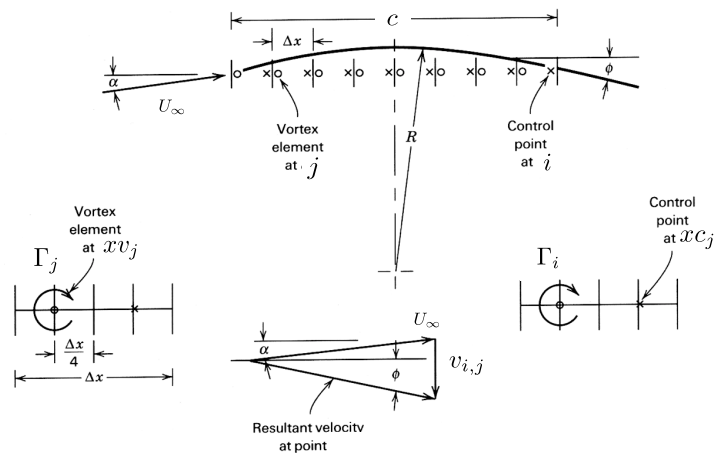
$$\frac{u}{U_\infty} = \left\{ 1 + \left[ \frac{dy_t}{dx} \right]^2 \right\}^{-1/2} \left( 1 + \frac{1}{\pi} \int_0^c \frac{dy_t(\xi)}{dx} \frac{d\xi}{x-\xi} \right)$$

The first term (the correction)  $\rightarrow 0$  as  $dy_t/dx \rightarrow \infty$ .

## Discrete direct methods for thin airfoils — 1

Now consider the discrete equivalent to finding the direct thin-airfoil continuum solution: given a camber line of arbitrary shape, determine the vorticity distribution, lift, moment...

1. Break the **chord** line up into  $N$  line segments. We place a discrete vortex of strength  $\Gamma$  at the  $1/4$ -chord point of each segment and a control point (where we determine velocity) at the  $3/4$ -chord point.



2. The *downward* velocity induced at the  $i$ th control point located at  $x_{ci}$  by the  $j$ th discrete vortex of strength  $\Gamma_j$  located at  $xv_j$  is

$$v'_{i,j} = \frac{\Gamma_j}{2\pi(x_{ci} - xv_j)}$$

$$\text{(recall } u_\theta = -\frac{\Gamma}{2\pi r} \text{ for potential flow)}$$

NB: vortices and control points are located on the chord line, just as in the continuous case.

## Discrete direct methods for thin airfoils – 2

3. The vector sum of the total induced vertical velocity and the oncoming flow has to be tangent to the **camber line** at each control point location  $i$ , as stated by

Each control point  $i$  generates one equation.

$$\sum_{j=1}^N \frac{\Gamma_j}{2\pi[xc_i - xv_j]} = U_\infty \left[ \alpha - \frac{dy_c}{dx} \Big|_i \right]$$

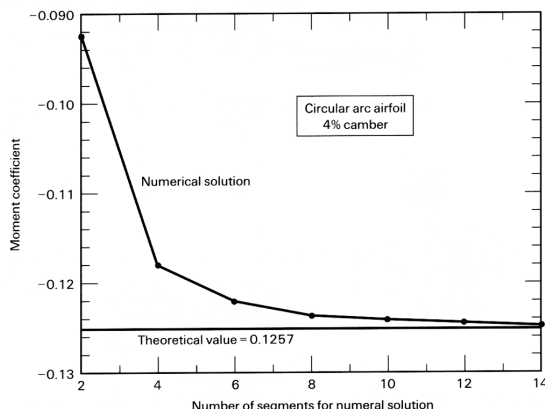
This is the discrete version of the flow tangency condition.

4. This gives  $N$  simultaneous linear equations that we can solve for the unknown  $\Gamma_j$ s.

5. From these we can obtain lift and moment coefficients, etc:

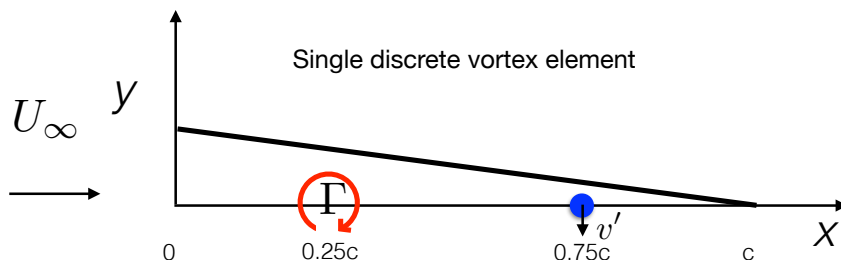
$$C_l = \frac{2}{U_\infty c} \sum_{i=1}^N \Gamma_i, \quad C_{m_{LE}} = -\frac{2}{U_\infty c^2} \sum_{i=1}^N xv_i \Gamma_i, \quad C_{m_{c/4}} = C_{m_{LE}} + C_l/4$$

6. These converge to the continuous solution as  $N \rightarrow \infty$ .



In fact for the particular locations of vortex and control points used, we get the exact  $C_l$ , regardless of  $N$  (including  $N=1$ , i.e. just one vortex), provided the camber line is continuous at  $0.75c$ .

## Easy example: flat plate



Velocity induced at collocation point

$$v'_{i,j} = \frac{\Gamma_j}{2\pi(xc_i - xv_j)} \longrightarrow v' = \Gamma/2\pi(0.5c)$$

Flow tangent to flat plate

$$v' = U_\infty \alpha \longrightarrow \Gamma = \pi U_\infty \alpha c$$

Lift coefficient

$$C_l = \frac{2}{U_\infty c} \Gamma = 2\pi\alpha$$

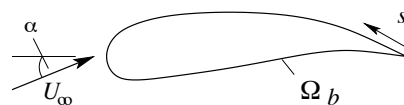
This result matches the theoretical result, but this only occurs with this trivial example. A higher number of vortices and control points is usually required for different cambers.

## 2D Panel Method: direct method – 1

Now we consider the problem of directly computing the potential flow without thin-airfoil assumptions.

- We consider potential flows governed by the Laplace equation with ‘no flow through’ boundary conditions at surfaces.

$$\nabla^2 \phi = 0 \quad \text{in } \Omega; \quad \mathbf{V} \cdot \mathbf{n} = \frac{\partial \phi}{\partial n} = 0 \quad \text{on } \Omega_b$$



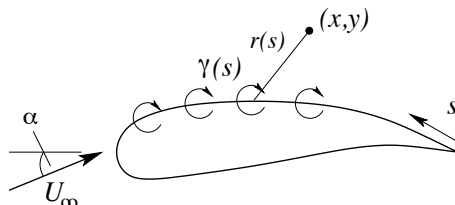
- Also we have to satisfy the Kutta condition, so that the flow leaves tangentially at the TE, or, if the TE angle is finite, at the average tangency.

- The solution is obtained by linearly superimposing basic solutions, for example vortex flow, which has (in  $r$ - $\theta$  polar coordinates):

$$\phi = -\frac{\Gamma}{2\pi} \theta; \quad \psi = \frac{\Gamma}{2\pi} \ln r; \quad v_\theta = -\frac{\Gamma}{2\pi r}; \quad v_r = 0.$$

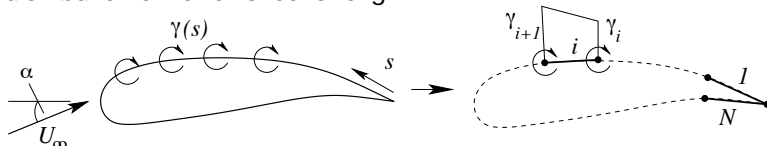
- Assuming a distribution of vortex sheet strength  $\gamma(s)$  along the perimeter length  $s$  of the airfoil, the velocity potential at any location corresponding to an incidence  $\alpha$  is

$$\phi(x, y) = U_\infty(x \cos \alpha + y \sin \alpha) - \frac{1}{2\pi} \oint \gamma(s) \arctan \left( \frac{y - y(s)}{x - x(s)} \right) ds$$



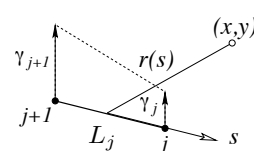
## 2D Panel Method: direct method – 2

- To calculate the integral approximately, divide the airfoil surface into  $N$  discrete panels, with piecewise-linear distribution of vortex sheet strength



The vortex sheet strength on a single panel is

$$\gamma(s_j) = \gamma_j + (\gamma_{j+1} - \gamma_j) \frac{s_j}{L_j}$$



- We add up all the contributions to velocity potential and then differentiate to obtain velocities.

- By imposing zero flow normal to the airfoil at a set of  $N$  control points we obtain  $N$  equations

$$\sum_{j=1}^N K_{ij} \gamma_j = \mathbf{U}_\infty \cdot \mathbf{n}_i \quad i = 1, 2, \dots, N$$

Here we have  $N$  equations and  $N+1$  unknowns (values of  $\gamma_j$ ). The influence coefficients  $K_{ij}$  are obtained from the integrals above.

- An additional equation that closes the system is obtained from the Kutta condition by adding an equation for the TE strengths

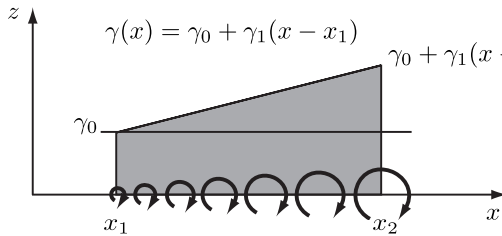
$$\gamma_1 + \gamma_{N+1} = 0$$

In continuum mechanics, panel methods are called ‘boundary element methods’  
– a special kind of finite element method.

## 2D Panel Method: direct method – 3

Details for linear-strength vortex panel (Katz & Plotkin chapters 10, 11, Kuettel & Chow chapter 5).

1. Start in panel coordinate system, vortex sheet strength  $\gamma(x)$ .



$$\phi(x, z) = -\frac{\gamma_0}{2\pi} \int_{x_1}^{x_2} \tan^{-1} \left( \frac{z}{x-x_0} \right) dx_0 - \frac{\gamma_1}{2\pi} \int_{x_1}^{x_2} x_0 \tan^{-1} \left( \frac{z}{x-x_0} \right) dx_0$$

2. Integrate to obtain:

$$\begin{aligned} \phi(x, z) = & -\frac{\gamma_0}{2\pi} \left[ (x-x_1) \tan^{-1} \left( \frac{z}{x-x_1} \right) - (x-x_2) \tan^{-1} \left( \frac{z}{x-x_2} \right) + \frac{z}{2} \ln \frac{(x-x_1)^2 + z^2}{(x-x_2)^2 + z^2} \right] \\ & - \frac{\gamma_1}{2\pi} \left[ \frac{xz}{2} \ln \frac{(x-x_1)^2 + z^2}{(x-x_2)^2 + z^2} - \frac{z}{2}(x_1-x_2) + \frac{x^2 - x_1^2 - z^2}{2} \tan^{-1} \left( \frac{z}{x-x_1} \right) - \frac{x^2 - x_2^2 - z^2}{2} \tan^{-1} \left( \frac{z}{x-x_2} \right) \right] \end{aligned}$$

$$r_1 = \sqrt{(x-x_1)^2 + z^2}, \quad \theta_1 = \tan^{-1} \frac{z}{x-x_1}$$

3. Let  $r_2 = \sqrt{(x-x_2)^2 + z^2}, \quad \theta_2 = \tan^{-1} \frac{z}{x-x_2}$

$\gamma_a = \gamma_0, \quad \gamma_b = \gamma_0 + \gamma_1(x_2 - x_1)$

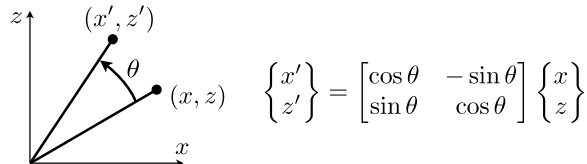
4. Differentiate the velocity potential to obtain panel-induced velocity components  $(u_p, w_p)$  at control point location  $(x_c, z_c)$ :

$$\begin{aligned} u_p &= \frac{z_c}{2\pi} \left( \frac{\gamma_b - \gamma_a}{x_2 - x_1} \right) \ln \frac{r_2}{r_1} + \frac{\gamma_a(x_2 - x_1) + (\gamma_b - \gamma_a)(x_c - x_1)}{2\pi(x_2 - x_1)} (\theta_2 - \theta_1), \\ w_p &= \frac{\gamma_a(x_2 - x_1) + (\gamma_b - \gamma_a)(x_c - x_1)}{2\pi(x_2 - x_1)} \ln \frac{r_2}{r_1} + \frac{z_c}{2\pi} \left( \frac{\gamma_b - \gamma_a}{x_2 - x_1} \right) \left[ \frac{x_2 - x_1}{z_c} + (\theta_1 - \theta_2) \right] \end{aligned}$$

## 2D Panel Method: direct method – 4

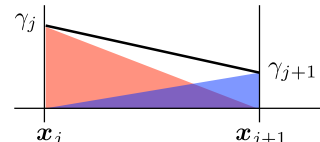
5. We need  $N$  panels to cover the airfoil. In general, for the  $j$ th panel, we can use the substitutions  $\gamma_a \rightarrow \gamma_j, \gamma_b \rightarrow \gamma_{j+1}, x_1 \rightarrow x_j, x_2 \rightarrow x_{j+1}, \theta_1 \rightarrow \theta_j, \theta_2 \rightarrow \theta_{j+1}$ .

6. The velocity components  $(u_p, w_p)$  were derived in the panel coordinate system. We need to transform/rotate both the given end points  $(x_j, z_j), (x_{j+1}, z_{j+1})$  for any panel as well as the collocation point of interest  $(x_i, z_i)$  from global to local coordinates, then transform the velocity components at any collocation point location back to global coordinates. Use direction cosine matrices:



7. We can break the collocation point velocity  $(u, w)(x_i, z_i)$  induced by the distribution of vorticity on panel  $j$  into two parts, each with a triangular shape function:

- (i)  $(u_a, w_a)(x_i, z_i) \leftarrow$  part related just to  $\gamma_j$
- (ii)  $(u_b, w_b)(x_i, z_i) \leftarrow$  part related just to  $\gamma_{j+1}$



8. Then implement all of the above via a subroutine that takes the  $j$ th panel end-coordinates  $(x_j, x_{j+1})$  and  $(x_{j+1}, z_{j+1})$  and the location of the  $i$ th control point  $(x_i, z_i)$ , and returns the global-coordinate velocity components  $(u_a, w_a)(x_i, z_i)$  and  $(u_b, w_b)(x_i, z_i)$  given unit strengths  $\gamma_j$  and  $\gamma_{j+1}$  for the panel-end vorticity distribution.

```
procedure vort2d1 (real      x1, z1, x2, z2, // -- panel-end coordinates
                  (real      xc, zc,           // -- collocation-point coordinates
                  (var real ua, wa, ub, wb) // -- output velocity components
```

## 2D Panel Method: direct method – 5

9. At the first control point there will be contributions from each of the panels:

$$(u, w)_1 = (u_a, w_a)_{1,1}\gamma_1 + [(u_b, w_b)_{1,1} + (u_a, w_a)_{1,2}]\gamma_2 + [(u_b, w_b)_{1,2} + (u_a, w_a)_{1,3}]\gamma_3 + \dots + [(u_b, w_b)_{1,N-1} + (u_a, w_a)_{1,N}]\gamma_N + (u_b, w_b)_{1,N}\gamma_{N+1}$$

And for the  $i$ th control/collocation point:

$$\begin{aligned} (u, w)_i &= (u_a, w_a)_{i,1}\gamma_1 + [(u_b, w_b)_{i,1} + (u_a, w_a)_{i,2}]\gamma_2 + [(u_b, w_b)_{i,2} + (u_a, w_a)_{i,3}]\gamma_3 + \dots + [(u_b, w_b)_{i,N-1} + (u_a, w_a)_{i,N}]\gamma_N + (u_b, w_b)_{i,N}\gamma_{N+1} \\ &= (u_a, w_a)_{i,1}\gamma_1 + \sum_{j=2}^N [(u_b, w_b)_{i,j-1} + (u_a, w_a)_{i,j}]\gamma_j + (u_b, w_b)_{i,N}\gamma_{N+1} \\ &\equiv \sum_{j=1}^{N+1} (u, w)_{i,j}\gamma_j \quad \text{This is one of a system of equations (a row in a matrix).} \end{aligned}$$

10. We want the not the velocity at the control points but the panel-normal component of the velocity (which we will set to zero):  $K_{i,j} = (u, w)_{i,j} \cdot \mathbf{n}_i$  where  $\mathbf{n}_i$  is the unit outward normal at control point  $i$ .

11. For each control point, the sum of the induced normal velocities has to be equal and opposite to the normal component of the free-stream velocity,  $\mathbf{U}_\infty = (u_\infty, w_\infty)$ :  $\text{RHS}_i = -(u_\infty, w_\infty) \cdot \mathbf{n}_i$

12. So far there are  $N$  equations but  $N+1$  unknowns. The Kutta condition gives closure:  $\gamma_1 + \gamma_{N+1} = 0$

13. Finally we have:

‘Influence coefficient’ matrix

$$\begin{bmatrix} K_{1,1} & K_{1,2} & \dots & K_{1,N+1} \\ K_{2,1} & K_{2,2} & \dots & K_{2,N+1} \\ \vdots & \vdots & \ddots & \vdots \\ K_{N,1} & K_{N,2} & \dots & K_{N,N+1} \\ 1 & 0 & \dots & 1 \end{bmatrix} \begin{Bmatrix} \gamma_1 \\ \gamma_2 \\ \vdots \\ \gamma_N \\ \gamma_{N+1} \end{Bmatrix} = \begin{Bmatrix} -(u_\infty, w_\infty) \cdot \mathbf{n}_1 \\ -(u_\infty, w_\infty) \cdot \mathbf{n}_2 \\ \vdots \\ -(u_\infty, w_\infty) \cdot \mathbf{n}_N \\ 0 \end{Bmatrix} \quad \text{which we solve for } \gamma_1, \dots, \gamma_{N+1}.$$

## 2D Panel Method: direct method – 6

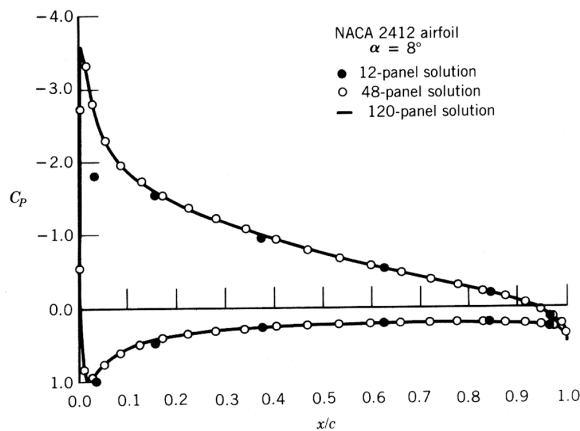
14. Once all the vorticities are known, the tangential velocity at each control point can be found:

$$U_{t,j} = (u_\infty, w_\infty) \cdot \mathbf{t}_j + (\gamma_j + \gamma_{j+1})/4 \quad \text{where } \mathbf{t}_j \text{ is the local panel tangent.}$$

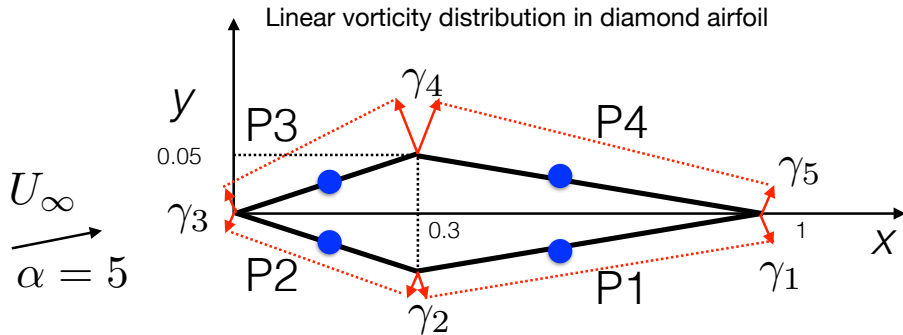
15. From this we can compute the pressure coefficient, contribution to lift, etc:

$$C_{p,j} = 1 - \frac{U_{t,j}^2}{U_\infty^2}; \quad \Delta L_j = \rho U_\infty \frac{\gamma_j + \gamma_{j+1}}{2} \Delta c_j$$

16. The solutions converge as we increase the  $N$ , the number of panels:



## 2D panel method example – 1



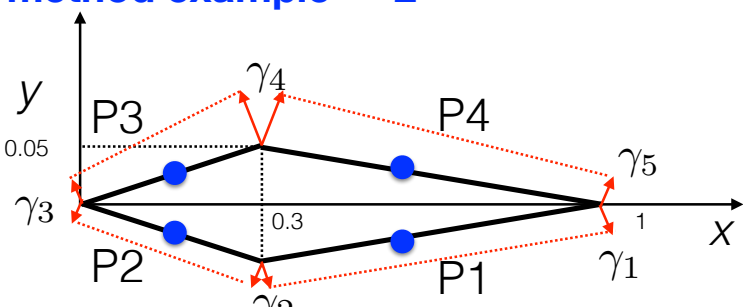
4 panels  $\rightarrow$  5x5 coefficient matrix

panel coordinates	control point	normal vector
(1,0)	(0.65,-0.025)	(0.0712,-0.9975)
(0.3,-0.05)	(0.15,-0.025)	(-0.1644,-0.9864)
(0,0)	(0.15,0.025)	(-0.1644,0.9864)
(0.3,0.05)	(0.65,0.025)	(0.0712,0.9975)
(1,0)		

## 2D panel method example – 2

Create first row of matrix corresponding to P1  
call **vort2dl** to obtain velocities in global coordinates

$(u_a, w_a)_1$
$(u_b, w_b)_1$



(-0.2606, 0.1409)	(0.0015, -0.055)	(-0.0038, -0.0444)	(-0.234, -0.112)	
	(-0.238, -0.1766)	(-0.0004, -0.0448)	(-0.0077, -0.0539)	(-0.2201, 0.1413)

Sum to obtain  $(u, v)_{1,j}$

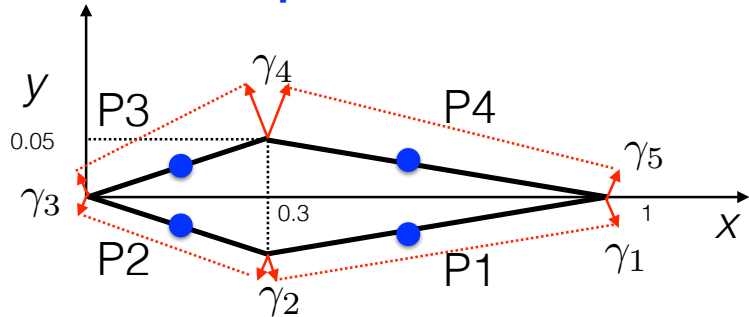
(-0.2606, 0.1409)	(-0.2365, -0.2316)	(-0.00384, -0.0892)	(-0.2347, -0.1659)	(-0.2201, 0.1413)
-------------------	--------------------	---------------------	--------------------	-------------------

Project onto normal vectors  $K_{i,j} = (u, v)_{i,j} \cdot \mathbf{n}_i$

$K_{1,j}$	-0.1592	0.2141	0.0887	0.1482	-0.1566
-----------	---------	--------	--------	--------	---------

## 2D panel method example – 3

Similarly for the next 3 rows



$K_{2,j}$	-0.0988	-0.3339	0.3081	-0.1892	-0.0956
$K_{3,j}$	0.0956	0.1892	-0.3081	0.3339	0.0988
$K_{4,j}$	0.1566	-0.1482	-0.0887	-0.2141	0.1592

Last row of matrix corresponds to Kutta condition  $\gamma_1 + \gamma_5 = 0$

$K_{5,j}$	1	0	0	0	1
-----------	---	---	---	---	---

## 2D panel method example – 4

Assembled influence coefficient matrix

Symmetry properties stem from airfoil symmetry.

-0.1592	0.2141	0.0887	0.1482	-0.1566
-0.0988	-0.3339	0.3081	-0.1892	-0.0956
0.0956	0.1892	-0.3081	0.3339	0.0988
0.1566	-0.1482	-0.0887	-0.2141	0.1592
1	0	0	0	1

Generate RHS vector by projecting free stream velocity onto normals  $-(U_\infty, W_\infty) \cdot \mathbf{n}_i$

$b$	0.016	0.2497	0.0778	-0.1579	0
-----	-------	--------	--------	---------	---

Solve linear system  $K\gamma = b$

$\gamma$	-0.8862	-0.9905	0.4848	1.233	0.8862
----------	---------	---------	--------	-------	--------

Compute velocities in panels  $U_{t,j} = (u_\infty, w_\infty) \cdot \mathbf{t}_j + (\gamma_j + \gamma_{j+1})/4$

Compute pressure coefficients and lift  $C_{p,j} = 1 - \frac{U_{t,j}^2}{U_\infty^2}; \quad \Delta L_j = \rho U_\infty \frac{\gamma_j + \gamma_{j+1}}{2} \Delta c_j$

$$C_l = 0.53884$$

## 2D Panel Method: inverse problem

Find the coordinates  $(x_j, y_j)$ ,  $j=1, \dots, N$  of points on the airfoil surface that produce a given distribution of pressure/velocity (i.e. vorticity)

Say we are given the pressure distribution on all panels,  $C_{p,j}$ . Since the average tangential velocity perturbation on each panel is half its average vorticity (as for thin airfoil theory), we have, for linear vorticity distribution

$$C_{p,j} = 1 - \left[ \frac{U_\infty \cos(\alpha + \alpha_j) + 0.25(\gamma_j + \gamma_{j+1})}{U_\infty} \right]^2 ; \quad j = 1, \dots, N$$

$\alpha_j$  is the panel angle relative to chord line  
Kutta condition at TE

$$\gamma_1 + \gamma_{N+1} = 0$$

which could be used to find all the vorticities provided we know the  $\alpha_j$ s (i.e. the airfoil shape).

However, the influence coefficients  $K_{ij}$  are nonlinear functions of the coordinates  $(x_j, y_j)$ . The solution requires an iterative procedure.

*Method of Kennedy and Marsden, J Aircraft 15 1978* (fixed point iteration):

The ordinates  $x_j$ ;  $j=1, \dots, N$  are given, and starting from an initial guess (a ‘seed airfoil’)  $y_j(0)$ ;  $j=1, \dots, N$ , the iteration for the  $y$ -coordinates is

$$y_j^{(n+1)} = \frac{1}{U_\infty \cos \alpha} \left[ \psi_0 + \sum_{j=1}^N K_{ij}^{(n)} \gamma_j \right] + x_j \tan \alpha$$

This is iterated until the coordinates converge.

## Boundary layer modelling

# Analysis of boundary layers – time-average

1. Introduction to BLs: laminar and turbulent flows, transition.
2. BL analysis: simplifying assumptions, formulation and solution methods.
  - i) differential form
  - ii) integral form

In the flow past an airfoil, viscous effects are mainly confined to a thin layer close to the surface of the airfoil (the *boundary layer*) and its wake.

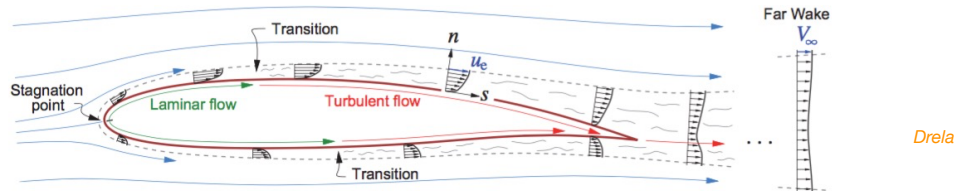


Figure 4.1: Boundary layer and wake development on a typical airfoil, shown by the  $u(n)$  velocity profiles. The layer thicknesses are shown exaggerated.

## Two important points about BL pressure

1. External to the BL, the flow is effectively inviscid and we can use Bernoulli's equation.

In streamline ( $s$ ) coordinates external to airfoil,  $p_\infty + \frac{1}{2}\rho V_\infty^2 = p(s) + \frac{1}{2}\rho u_e^2(s) = \text{const.}$

2. Since airfoil boundary layers are typically very thin in relation to their radius of curvature

$$\begin{aligned} -\frac{dp}{ds} &= u_e \frac{du_e}{ds} \\ \frac{\partial p}{\partial n} &\approx 0 \end{aligned}$$

I.e. BL pressure is that in the external inviscid flow just outside BL, related to flow speed gradient, and constant in wall-normal direction.

MAE4409

## Boundary layer modelling: PDE form

For 2D steady/time-average incompressible flow, with  $u \sim U_e$ ,  $p \sim \rho U_e^2$ ,  $s \sim c$ ,  $n \sim \delta$  assuming  $\delta \ll c$ ,  $Re \gg 1$ , then  $\partial/\partial n \gg \partial/\partial s$  and the N-S equations simplify to 'BL equations':

$$\begin{aligned} \frac{\partial u}{\partial s} + \frac{\partial v}{\partial n} &= 0 \\ \rho \left( u \frac{\partial u}{\partial s} + v \frac{\partial u}{\partial n} \right) &= -\frac{\partial p}{\partial s} + \frac{\partial \tau_{ss}}{\partial s} + \frac{\partial \tau_{sn}}{\partial n} \\ \rho \left( u \frac{\partial v}{\partial s} + v \frac{\partial v}{\partial n} \right) &= -\frac{\partial p}{\partial n} + \frac{\partial \tau_{ns}}{\partial s} + \frac{\partial \tau_{nn}}{\partial n} \end{aligned} \Rightarrow \begin{aligned} \frac{\partial u}{\partial s} + \frac{\partial v}{\partial n} &= 0 \\ u \frac{\partial u}{\partial s} + v \frac{\partial u}{\partial n} &= U_e \frac{\partial U_e}{\partial s} + \frac{1}{\rho} \frac{\partial \tau}{\partial s} \\ \frac{\partial p}{\partial n} &= 0 \end{aligned}$$

Important: unlike the NSE and potential flows, which generate elliptic PDEs, the BL equations are 'parabolic' PDEs and are integrated/marched forward in  $s$ , given an inlet/LE BC. Also, we must be given  $U_e$  in advance.

Laminar flow  $\tau = \mu \frac{\partial u}{\partial n}$

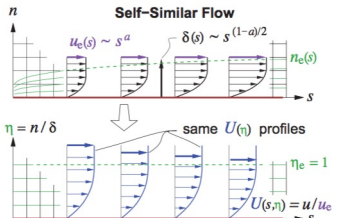
Turbulent flow  $\tau = \mu \frac{\partial u}{\partial n} - \rho \bar{u}' v'$  and we need a model for the Reynolds stress  $\bar{u}' v'$

For the laminar case, assuming the two terms on the RHS of the momentum equation scale like (~)

$$U_e \frac{\partial U_e}{\partial s} \sim \frac{U_e^2}{s} \quad \text{and} \quad \frac{1}{\rho} \frac{\partial \tau}{\partial s} = \nu \frac{\partial^2 u}{\partial n^2} \sim \nu \frac{U_e}{\delta^2} \quad \text{and are of similar magnitude: } \frac{U_e^2}{s} \sim \nu \frac{U_e}{\delta^2}$$

we obtain  $\delta \sim \sqrt{\frac{s\nu}{U_e}} = \frac{s}{\sqrt{Re_s}}$  or  $\frac{\delta}{s} \sim \frac{1}{\sqrt{Re_s}}$

## Similarity solutions for laminar BLs—1



1. Consider the laminar zero-pressure gradient (ZPG) BL (with  $U_e = \text{const}$ ). This is described by

$$\frac{\partial u}{\partial s} + \frac{\partial u}{\partial n} = 0, \quad u \frac{\partial u}{\partial s} + v \frac{\partial u}{\partial n} = \nu \frac{\partial^2 u}{\partial s^2}$$

2. We know from order of magnitude analysis that the BL thickness  $\delta \sim (sv/U_e)^{1/2}$ . The BL profile does not change shape in the streamwise direction when scaled w.r.t.  $\delta$ , i.e.  $u/U_e = \text{function}(n/\delta)$ . Instead of (dimensionless)  $n/\delta$  we could use  $\eta = n(U_e/2vs)^{1/2}$ ; the '2' for convenience later.

3. Next we introduce the streamfunction  $\psi = \int u dn |_{s=\text{const}}$  which should increase with  $\delta$  (i.e. as more fluid is entrained from the freestream into the BL), or equivalently with  $s^{1/2}$ . We write  $\psi = (2vU_e s)^{1/2} f(\eta)$  which is the dimensionally correct way of describing it in terms of  $\eta$ . Recall that with  $u = \partial \psi / \partial n$  and  $v = -\partial \psi / \partial s$  the flow will be incompressible. The velocity components are:

$$u = \frac{\partial \psi}{\partial n} = U_e f(\eta), \quad v = -\frac{\partial \psi}{\partial s} = \left( \frac{\nu U_e}{2s} \right)^{1/2} (\eta f' - f) \quad (f' \equiv df/d\eta)$$

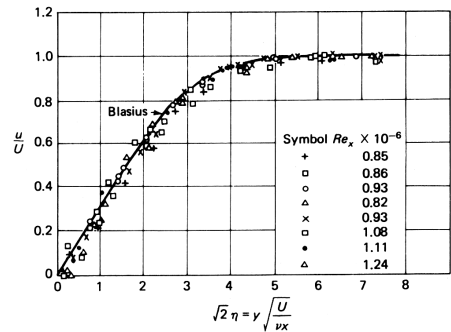
4. Upon substituting these forms into the momentum equation **Blasius (1908)** obtained

$$f''' + ff'' = 0$$

which we note is now an ODE rather than a PDE. The equation is solved subject to the BCs

$$f'(0) = f(0) = 0, \quad f'(\infty) = 1$$

The (numerical) solution to this equation agrees well with experimental results.



White

MAE4409

## Similarity solutions for laminar BLs—2

5. **Faulkner and Skan (1931)** showed that Blasius' similarity solution can be generalized if the freestream velocity  $U_e$  is a power-law function of  $s$ , i.e.  $U_e(s) = Ks^m$  in which case the similarity variable  $\eta = Cns^a$  with  $m = 2a + 1$ . Blasius' ZPG solution is the special case for  $m = 0$ .

The external pressure gradient is required to be  $\frac{dp}{ds} = -\rho U_e^2 \frac{m}{s}$

6. The similarity variable  $\eta$  now contains the exponent  $m$ :  $\eta = y \left( \frac{m+1}{2} \frac{U_e}{\nu s} \right)^{1/2}$

7. The result corresponding to Blasius' ODE is the Faulkner–Skan equation

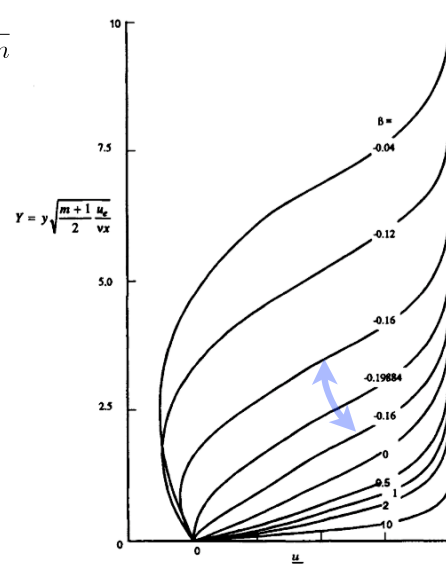
$$f''' + ff'' + \beta(1 - f^2) = 0, \quad \text{where} \quad \beta = \frac{2m}{1+m}$$

BCs are as before:  $f'(0) = f(0) = 0, \quad f'(\infty) = 1$

8. The equation is solved numerically. Stewartson (1954) pointed out that for  $\beta < 0$  there are a number of solution branches, some of which provide reversed flow near the wall (see e.g. two different solution curves for  $\beta = -0.16$ ).

Incipient flow separation corresponds to  $\beta = -0.19884$ , while Blasius' solution corresponds to  $\beta = 0$ .

A key point is that we have generalised the (Blasius) similarity solution for the zero-pressure-gradient BL, giving self-similar/equilibrium BL shapes as a function of pressure gradient and local skin friction coefficient.



White

MAE4409

## Modelling of turbulent BLs

1. Turbulent flow is chaotic/random, complicated, and varies in both space and time. Unlike some laminar flows (e.g. Blasius BL), turbulent flows cannot be solved in closed form.

2. Analyzing/modelling turbulent flows for engineering design is based in statistics and turbulence models that attempt to model fluctuating quantities in terms of their mean values.

3. BL turbulence (i.e. in attached BL flow) is somewhat easier to deal with than the general case.

4. Propose that any quantity can be decomposed into a mean value and a zero-mean fluctuation:

$$u = \bar{u} + u' \quad \bar{u} = \frac{1}{T} \int_0^T u dt \quad \text{The mean of a product: } \bar{uv} = \overline{(\bar{u} + u')(\bar{v} + v')} = \bar{u}\bar{v} + \overline{u'v'}$$

5. Noting that with the incompressibility constraint  $\frac{\partial u}{\partial s} + \frac{\partial v}{\partial n} = 0$  we have

6. Now we can write the time-mean BL momentum equation as  $u \frac{\partial u}{\partial s} + v \frac{\partial u}{\partial n} \equiv \frac{\partial uu}{\partial s} + \frac{\partial uv}{\partial n}$

$$\frac{\partial uu}{\partial s} + \frac{\partial uv}{\partial n} = U_e \frac{\partial U_e}{\partial s} + \frac{\mu}{\rho} \frac{\partial^2 u}{\partial n^2} \quad \rightarrow \quad \bar{u} \frac{\partial \bar{u}}{\partial s} + \bar{v} \frac{\partial \bar{u}}{\partial n} = U_e \frac{\partial U_e}{\partial s} + \frac{\mu}{\rho} \frac{\partial^2 \bar{u}}{\partial n^2} - \frac{\partial \bar{u}'v'}{\partial n}$$

7. The quantity  $\rho \overline{u'v'}$  is called a Reynolds stress in honour of Osborne Reynolds.

8. Trouble: the equation set is no longer closed because we introduced this new variable. The task of a turbulence model is to guess a relationship between the Reynolds stresses and the mean velocities, thus closing the set of equations.

9. The simplest workable approach is the mixing length model (due to Prandtl):  $-\overline{u'v'} = l_{\text{mix}} \left| \frac{\partial \bar{u}}{\partial n} \right| \frac{\partial \bar{u}}{\partial n}$

10. For a turbulent BL,  $l_{\text{mix}} = \kappa n$  where  $\kappa \approx 0.4$  is the von Karman constant.

In this case we have  $\tau(s, n) = \tau_l + \tau_t = (\mu + \mu_t(s, n)) \frac{\partial u}{\partial n}$

MAE4409

## Laminar vs turbulent BL

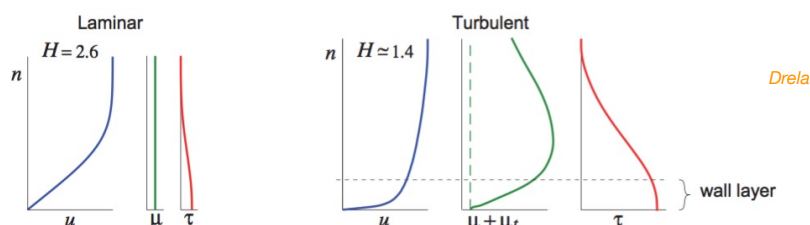
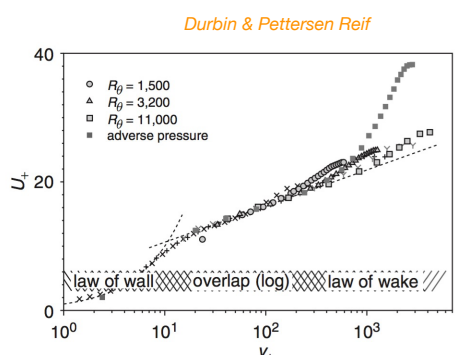


Figure 4.5: Comparison of laminar and turbulent flat-plate velocity, viscosity, and shear profiles. The shape parameter  $H$  is introduced in Section 4.5.

The key feature which makes turbulent boundary layers so different is that  $\mu_t$  is large relative to  $\mu$  over most of the turbulent boundary layer, but falls linearly to zero over roughly the bottom 20% portion called the *wall layer*. Here the total stress  $\tau$  is approximately constant and equal to the wall shear stress  $\tau_w$ . Hence in the wall layer  $\partial u / \partial n$  varies roughly as  $1/n$ , and therefore  $u(n) \sim \ln n$ . The variation of all the quantities in the wall layer can be summarized as follows.

$$\begin{aligned} \tau(n) &\simeq \tau_w \sim \text{const.} \\ \mu_t(n) &\sim n \\ \frac{\partial u}{\partial n} &= \tau(n)/\mu_t(n) \sim 1/n \quad (\text{assuming } \mu \ll \mu_t) \\ u(n) &\sim \ln n \end{aligned}$$

This is a robust feature of equilibrium turbulent boundary layer profiles: they have logarithmic shape over some portion (close to the wall, but not all the way). True for all kinds of external pressure gradients (see e.g. Coles 1956).

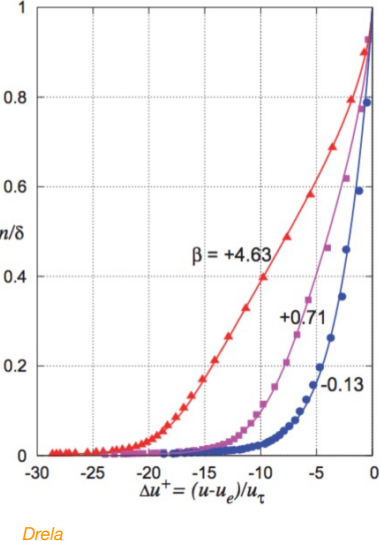
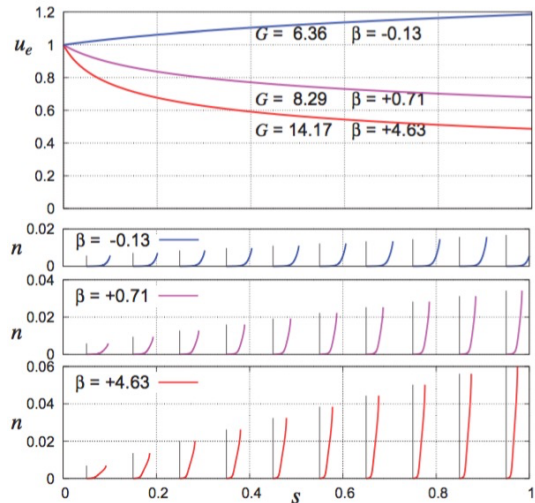


## Self-similar turbulent BLs

Just like laminar BLs with carefully controlled external pressure gradients, turbulent BLs can take self-similar (a.k.a. equilibrium) shapes for zero, adverse and favourable pressure gradients of suitable streamwise variation (Clauser 1954).

In this case the appropriate form of the dimensionless velocity profile is the velocity defect normalised by the ‘friction velocity’ which is a measure of the wall shear traction  $\tau_w$ . We plot

$$\Delta u^+ = \frac{u(s, n) - U_e(s)}{u_\tau} \quad \text{where} \quad u_\tau = \sqrt{\frac{\tau_w}{\rho}} \quad \text{vs} \quad \eta(s, n) = \frac{n}{\delta(s)}$$



$\beta$  and  $G$  are parameters of the self-similar shape, pressure gradient, skin friction.

$\beta = 0$  gives the standard ZPG turbulent BL.

$\beta > 0$  corresponds to an adverse pressure gradient while  $\beta < 0$  corresponds to a favourable gradient.

$$\Delta u^+(0) = -\sqrt{\frac{2}{c_f}}$$

MAE4409

## Finite differences (FD) solution of the BL equations

We note that in principle, solutions to both laminar and turbulent mean-flow BL PDEs can be approximated numerically using grid-based methods (e.g. finite differences). (In practice this is rarely done owing to expense of calculation.)

Reminder: since the BL PDEs are parabolic in nature, they can be ‘marched’ downstream, starting from initial upstream data.

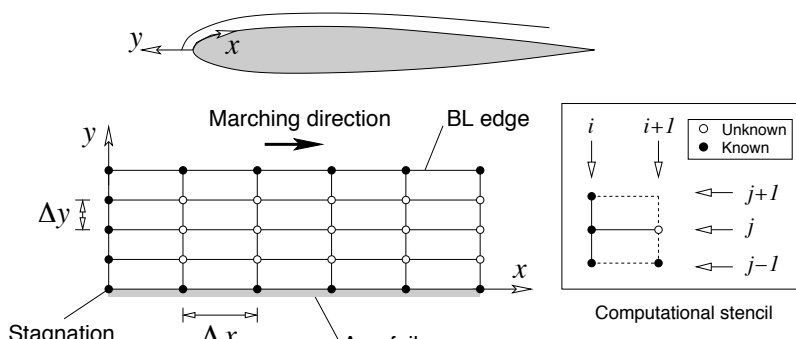
Here is a simple method that employs forward differences in  $x$  and central differences in  $y$ :

<b>PDEs:</b> $u \frac{\partial u}{\partial x} + v \frac{\partial u}{\partial y} = \frac{1}{2} \frac{dU_e^2}{dx} + \nu \frac{\partial^2 u}{\partial y^2} \rightarrow u_{i,j} \frac{u_{i+1,j} - u_{i,j}}{\Delta x} + v_{i,j} \frac{u_{i,j+1} - u_{i,j-1}}{2\Delta y} =$ $\frac{U_e _{i+1} - U_e _i}{2\Delta x} + \nu \frac{u_{i,j+1} - 2u_{i,j} + u_{i,j-1}}{\Delta y^2}$ $\frac{\partial u}{\partial x} + \frac{\partial v}{\partial y} = 0 \rightarrow \frac{u_{i+1,j} - u_{i,j}}{\Delta x} + \frac{v_{i+1,j} - v_{i+1,j-1}}{\Delta y} = 0$	<b>FDEs:</b> $u_{i,j} \frac{u_{i+1,j} - u_{i,j}}{\Delta x} + v_{i,j} \frac{u_{i,j+1} - u_{i,j-1}}{2\Delta y} =$ $\frac{U_e _{i+1} - U_e _i}{2\Delta x} + \nu \frac{u_{i,j+1} - 2u_{i,j} + u_{i,j-1}}{\Delta y^2}$ $\frac{u_{i+1,j} - u_{i,j}}{\Delta x} + \frac{v_{i+1,j} - v_{i+1,j-1}}{\Delta y} = 0$
---	---

A single streamwise step consists of:

1. March this in  $x$  to obtain  $u_{i+1,j}$  from  $u_{i,j}$ .

2. March this in  $y$  to obtain  $v_{i+1,j}$  from  $v_{i+1,j-1}$ .



## FD: difficulties

1. Requires a (good) solution at the inflow to be known (e.g. Hiemenz stagnation flow)
2. Stability: this particular FD approximation is explicit and for stability requires

$$\Delta x < \frac{u_{\min} \Delta y^2}{2\nu} \quad \text{and} \quad \Delta y < \frac{2\nu}{|v_{\max}|}$$

*Problem:*  $u_{\min}$  approaches zero near the wall and this imposes severe restrictions in the size  $\Delta x$ . Reducing  $\Delta x$  increases the cost.

*Solution:* use an implicit method, more complicated, but stable.

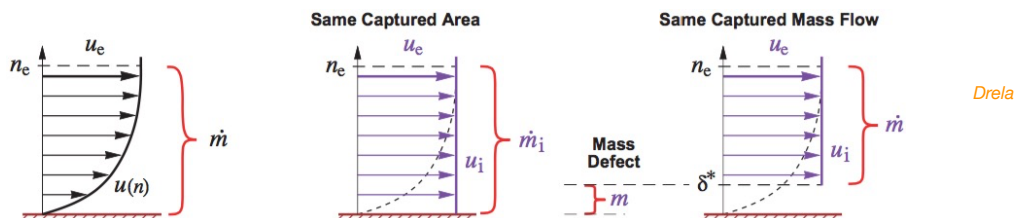
3. The location of the BL edge (largest  $\delta$ ) must be known (or guessed) for mesh design
4. Unsuitable for separated flow: recirculation does not allow for a marching direction

In practice, wall-normal integrated forms of the BL equations (which produces ODEs from PDEs) are typically used for modelling aeronautical BL flows, instead of discretising the BL PDEs and solving them on a grid of points.

## Defect integrals and thicknesses

In the following,  $u_i$  is the inviscid external inviscid flow speed  $u_e$  carried down to the wall. And  $n_e$  is the wall-normal distance to the edge of the BL.

**Mass flow comparison** between the true viscous flow and the “equivalent inviscid flow”



$$\text{mass flow rate per unit span} \quad \dot{m} = \int d\dot{m} = \int_0^{n_e} \rho u \, dn = \int_0^{n_e} \rho_e u_e \, dn - \int_0^{n_e} (\rho_e u_e - \rho u) \, dn$$

$$\text{or} \quad \boxed{\dot{m} = \dot{m}_i - m}$$

$$\begin{aligned} \text{where} \quad \dot{m}_i &\equiv \int_0^{n_e} \rho_e u_e \, dn = \rho_e u_e n_e \\ m &\equiv \int_0^{n_e} (\rho_e u_e - \rho u) \, dn = \rho_e u_e \delta^* \quad \text{mass flow defect} \\ \text{and} \quad \delta^* &\equiv \int_0^{n_e} \left(1 - \frac{\rho u}{\rho_e u_e}\right) \, dn \quad \text{displacement thickness} \end{aligned}$$

## Defect integrals and thicknesses

### Momentum and kinetic energy flow (force and power) comparisons

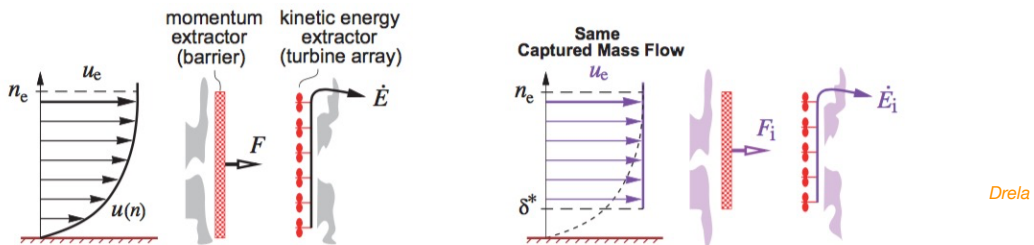


Figure 4.3: Comparison of actual and EIF's momentum flow and kinetic energy flow, for the same mass flow. Momentum flow is equal to the force on a hypothetical barrier which brings the fluid stream's  $s$ -velocity to zero. Kinetic energy flow is equal to the power from an ideal turbine array which brings the fluid stream's velocity to zero reversibly.

$$\begin{aligned} \text{momentum flow per unit span} \quad F &= \int u \, dm = \int_0^{n_e} \rho u^2 \, dn = \int_0^{n_e} \rho_e u_e^2 \, dn - u_e \int_0^{n_e} (\rho_e u_e - \rho u) \, dn - \int_0^{n_e} (u_e - u) \rho u \, dn \\ &= \rho_e u_e^2 n_e - u_e (\rho_e u_e \delta^*) - \rho_e u_e^2 \theta \\ &\boxed{F = F_i - P} \end{aligned} \quad (4.7)$$

$$\begin{aligned} \text{energy flow per unit span} \quad \dot{E} &= \int \frac{1}{2} u^2 \, dm = \int_0^{n_e} \frac{1}{2} \rho u^3 \, dn = \int_0^{n_e} \frac{1}{2} \rho_e u_e^3 \, dn - \frac{1}{2} u_e^2 \int_0^{n_e} (\rho_e u_e - \rho u) \, dn - \int_0^{n_e} \frac{1}{2} (u_e^2 - u^2) \rho u \, dn \\ &= \frac{1}{2} \rho_e u_e^3 n_e - \frac{1}{2} u_e^2 (\rho_e u_e \delta^*) - \frac{1}{2} \rho_e u_e^3 \theta^* \\ &\boxed{\dot{E} = \dot{E}_i - K} \end{aligned} \quad (4.8)$$

## Defect integrals and thicknesses

### Integral defects and associated thicknesses

$$\begin{aligned} P &\equiv \int_0^{n_e} (u_e - u) \rho u \, dn = \rho_e u_e^2 \theta && \text{(momentum defect)} \\ K &\equiv \int_0^{n_e} \frac{1}{2} (u_e^2 - u^2) \rho u \, dn = \frac{1}{2} \rho_e u_e^3 \theta^* && \text{(kinetic energy defect)} \\ \theta &\equiv \int_0^{n_e} \left(1 - \frac{u}{u_e}\right) \frac{\rho u}{\rho_e u_e} \, dn && \text{(momentum thickness)} \\ \theta^* &\equiv \int_0^{n_e} \left(1 - \frac{u^2}{u_e^2}\right) \frac{\rho u}{\rho_e u_e} \, dn && \text{(kinetic energy thickness)} \end{aligned}$$

For incompressible flows, the thickness quantities are just functions of BL shape. If  $\rho_e = \rho$ :

$$\delta^* = \int_0^{n_e} (1 - U) \, dn, \quad \theta = \int_0^{n_e} (U - U^2) \, dn, \quad \theta^* = \int_0^{n_e} (U - U^3) \, dn$$

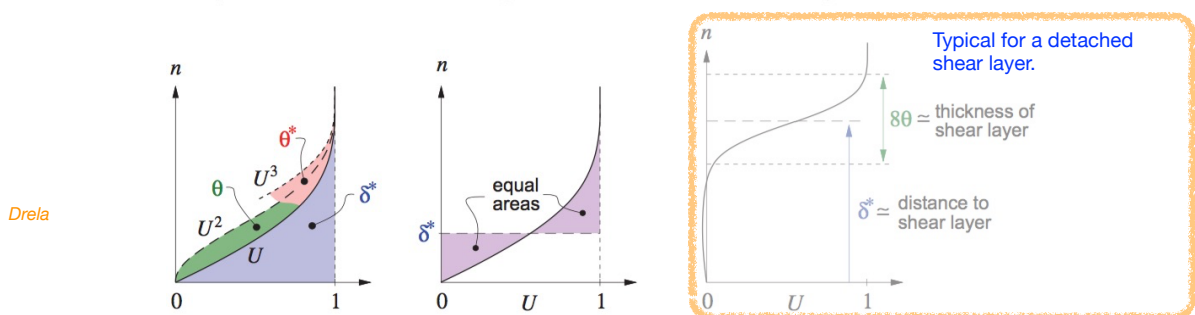


Figure 4.4: Interpretation of the integral thicknesses for incompressible flow, in terms of the geometry of the normalized velocity profile  $U = u/u_e$ , and also  $U^2$  and  $U^3$ . Since the horizontal scale is dimensionless, the areas have the same length unit as the vertical  $n$  axis.

## Boundary layer equations

Using the thin shear layer TSL approximations

$$\begin{aligned} v &\ll u \\ \frac{\partial u}{\partial s} &\ll \frac{\partial u}{\partial n} \quad \text{leads to} \\ \frac{\partial p}{\partial n} &\simeq 0 \end{aligned}$$

$$\bar{\tau} = \begin{bmatrix} \tau_{ss} & \tau_{sn} \\ \tau_{ns} & \tau_{nn} \end{bmatrix} \simeq \begin{bmatrix} 0 & \tau \\ \tau & 0 \end{bmatrix}$$

and the boundary layer equations

recall  $-\frac{\partial p}{\partial s} \approx \rho_e u_e \frac{du_e}{ds}$

$$\begin{aligned} \frac{\partial \rho u}{\partial s} + \frac{\partial \rho v}{\partial n} &= 0 \\ \rho u \frac{\partial u}{\partial s} + \rho v \frac{\partial u}{\partial n} &= \rho_e u_e \frac{du_e}{ds} + \frac{\partial \tau}{\partial n} \\ \tau &= (\mu + \mu_t) \frac{\partial u}{\partial n} \end{aligned}$$

continuity

s-component momentum

(this form for turbulent shear stress is an approximation only)

with boundary conditions

$$\begin{aligned} \text{at wall, } n=0 : \quad u &= 0, \quad v = 0 \\ \text{at edge, } n=n_e : \quad u &= u_e \end{aligned}$$

recall

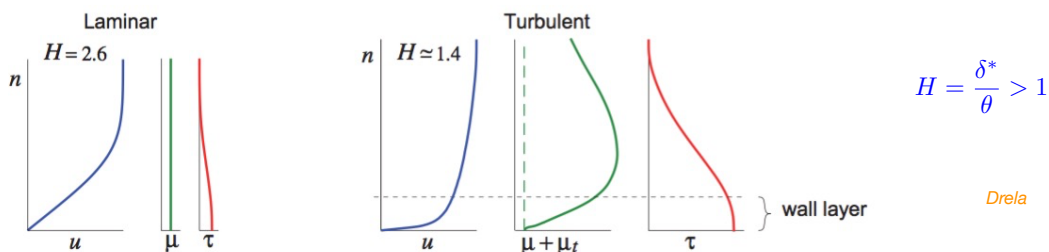


Figure 4.5: Comparison of laminar and turbulent flat-plate velocity, viscosity, and shear profiles.

## BL response to pressure and shear gradients

### Response to streamwise pressure gradients

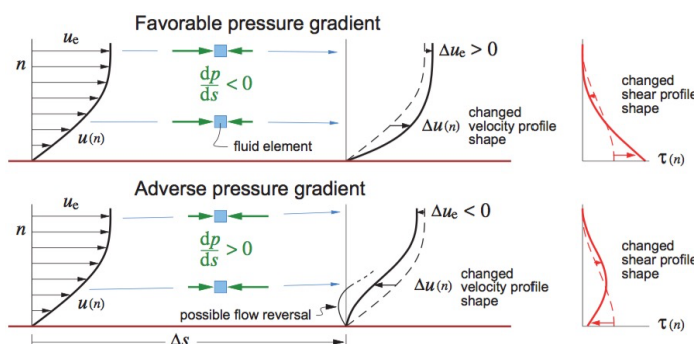


Figure 4.6: Velocity changes  $\Delta u$  along streamlines resulting from a favorable or adverse pressure gradient which applies the same accelerating or decelerating net force per unit volume to all fluid elements. Slower-moving elements have a larger  $\Delta u$ , resulting in a distortion of the velocity profile. A sufficiently strong adverse pressure gradient will cause a flow reversal and boundary layer separation.

### Response to wall-normal shear gradient

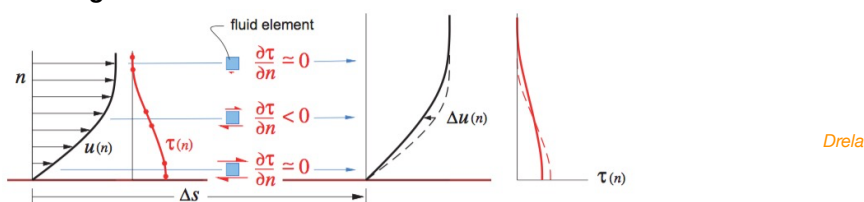


Figure 4.7: A transverse shear gradient produces a net streamwise force per unit volume which tends to "flatten" the velocity profile, and results in an overall growth of the boundary layer.